MIXING IN COMPRESSIBLE SHEAR LAYERS

A Thesis
Presented to
The Academic Faculty

by

Ratheesvar Mohan

In Partial Fulfillment
of the Requirements for the Degree
Bachelor of Science in Aerospace Engineering in the
Daniel Guggenheim School of Aerospace Engineering

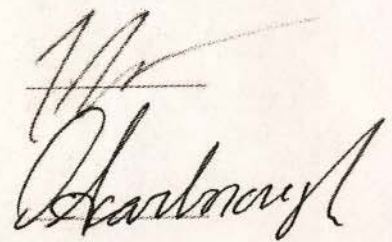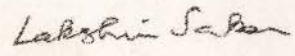Georgia Institute of Technology
May 2015

MIXING IN COMPRESSIBLE SHEAR LAYERS

Approved by:

Dr. Jeff Jagoda, Advisor
School of Aerospace Engineering
Georgia Institute of Technology

Dr. David Scarborough
School of Aerospace Engineering
Georgia Institute of Technology

Dr. Lakshmi Sankar
School of Aerospace Engineering
Georgia Institute of Technology

Date Approved: 04/30/2015

TABLE OF CONTENTS

Page

LIST OF TABLES

LIST OF FIGURES

LIST OF SYMBOLS AND ABBREVIATIONS

M_c	Convective Mach number
ΔU	Difference in velocities of primary and secondary streams
PLIF	Planar Laser Induced Fluorescence
a_1	Speed of sound in primary stream
a_2	Speed of sound in secondary stream
C	Discharge coefficient
$\dot{m}$	Mass flow rate
Y_1	Gas expansion factor
D_1	Pipe diameter
D_2	Bore diameter
β	Ratio of bore diameter to pipe diameter
ρ	Density of stream (primary or secondary)
ΔP	Differential pressure of stream (primary or secondary)
R_D	Reynold's number
μ	Viscosity
C_∞	Discharge coefficient at infinite Reynold's number

CHAPTER 1

INTRODUCTION

Hypersonic flight in the atmosphere, which has long been a sought after capability of the aerospace field, requires a propulsion system capable of operating at flight speeds. Supersonic combustion ramjets, or Scramjets, have historically been the preferred solution to this problem, owing to their reduced mechanical complexity and relatively high efficiency, especially in cruise conditions. However, to achieve supersonic combustion, which by definition is the basis of Scramjets, the air entering the combustion chamber, having undergone natural compression because of the geometry of the inlet, must mix effectively and efficiently with fuel in the limited chamber length available.

Although past research into mixing in compressible shear layers has established that the growth rate of the shear layer, where the majority of mixing occurs, decreases rapidly with the convective Mach number (especially below approximately 0.6)[1], the reasons for this occurrence have not been fully determined. In particular, the effect of compressibility on the efficiency of mixing has not been completely understood, although some studies have determined that the compressibility effects on mixing are less pronounced than the effects of velocity and density ratios.[2] Past studies have also shown that mixing efficiency improves with increasing Reynolds number, which is a flow parameter that describes the ratio of inertial to viscous forces.[3]

Mixing is usually quantified by measuring the concentration of either a particular substance in the shear layer or the product of a chemical reaction. Several studies have been conducted by measuring the former. This technique, known as the 'passive scalar'

1

technique requires imaging systems with a sufficiently high spatial resolution. The required resolution is on the order of the Batchelor scale, which describes the size of a droplet of the scalar in question.[4] Of the studies done thus far, several have utilized charge-coupled device (CCD) array cameras which did not have a sufficiently high spatial resolution.[5] Some of the misunderstanding of the effects of compressibility on mixing can be attributed to incorrect results obtained using such cameras.

Consequently, an opportunity exists for a more accurate study of mixing in compressible shear layers using the 'passive scalar' technique. This study investigated the effect of convective Mach number on the efficiency of mixing, on the order of the Batchelor scale. The results obtained will have direct implications for the determination of the effects of compressibility on mixing and may ultimately lead to the development of an efficient combustion system, and subsequently an efficient propulsion system, for supersonic vehicles.

CHAPTER 2

LITERATURE REVIEW

One of the most important parameters investigated by studies on mixing is the growth of the mixing rate of mixing layers with different variables such as the Mach number and the density ratio of the flows. This growth rate decreases exponentially with Mach number[6], as evidenced in Figure 1. Further, as Brown and Roshko showed in their study of density effects turbulent mixing layers, in compressible shear layers, the growth rate is approximately one fourth of the growth in incompressible shear layers with similar density ratios.[7]

Even though the variation of the mixing layer growth rate with Mach number has been the subject of several studies, a more relevant Mach number to mixing studies is the convective Mach number (introduced by Bogdanoff in 1983), which is essentially a measure of the convection velocity of large-scale motions in the mixing layer relative to the average speed of sound in the flows on either side of the mixing layer (the primary and secondary flows).[8] Therefore, this Mach number is defined as

Figure 1: Mixing layer growth rate with Mach number.[6]

$$M_c = \frac{\Delta U}{a_1 + a_2}$$

Two commonly used techniques to quantify mixing are the 'passive scalar' and 'cold chemistry' techniques. The latter technique is used as an alternative to chemical product methods requiring fast chemistry and has been used extensively by Island (1997) and by Clemens and Paul (1995).[3] Rossmann et al. used a modified version of the traditional cold chemistry technique which yielded more accurate results than the traditional technique which tended to under-predict the quantity of mixed fluid.[3] They confirmed the results of prior cold chemistry experiments by showing that mixing efficiency improves with Reynolds number (for Reynolds numbers higher than 1×10^5) and with increasing compressibility. While this study justifies its very robust methodology well and provides a clear context in which its results may be interpreted, experiments were conducted only at one specific convective Mach number (2.64) and hence are not widely applicable.

Contradicting the conclusions of Rossmann et al., Bonanos et al.[9] found mixing efficiency to decrease with increasing convective Mach number. Using a chemical product technique based on the hypergolic hydrogen-fluorine reaction with an expansion-ramp configuration, it was shown that mixing was higher than in free shear layers.

Despite the several studies of mixing that have been performed using a variety of techniques, a definitive trend has not been established for the variation of mixing efficiency with convective Mach number. Bonanos et al.[9] reported an inversely proportional relationship while Rossman et al.[3] reported a proportional one. Yet others, such as Island et al.[10], also utilizing a cold chemistry technique, reported no change or a slight increase in mixing, which may have been a result of increasing Reynolds number and not increasing convective Mach number. A summary of the findings of the

4
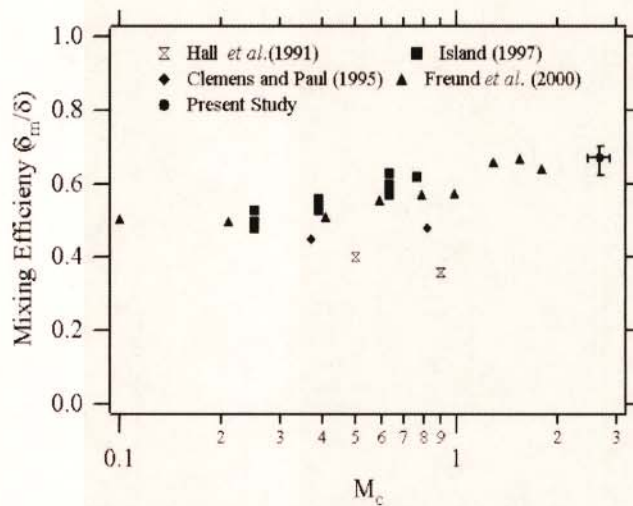
Figure 2: Variation of mixing efficiency with convective Mach number[3]

aforementioned studies is provided in Figure 2. The reasons for these widely differing results is not fully understood, although it may be attributed to a combination of several factors such as ambiguous distinguishing of compressibility effects from Reynolds number effects, differences between axisymmetric and planar shear layers and limitations of the measurement techniques used. Passive scalar techniques require very high spatial resolution, the magnitude of which is dictated by the Batchelor scale.[4] Experiments performed with insufficient spatial resolution tend to under-predict the quantity of mixed fluid, or mixing efficiency. Chemical product techniques require fast chemistry, which can lead to inaccurate predictions of mixing efficiency at supersonic speeds where chemical time scales are not as fast, relatively, when compared to fluid mechanical time scales.[11]

This study employed a passive scalar technique and use imaging devices with sufficient spatial resolution, thus enabling measurements on the order of the Batchelor scale. The experiments wer repeated at different convective Mach numbers, ranging from 0.1 to 1.3, with the goal of determining and understanding the effects of compressibility on molecular mixing and the underlying mechanisms thereof, specifically in supersonic shear layers.

5

CHAPTER 3

METHODS AND MATERIALS

Experimental Setup
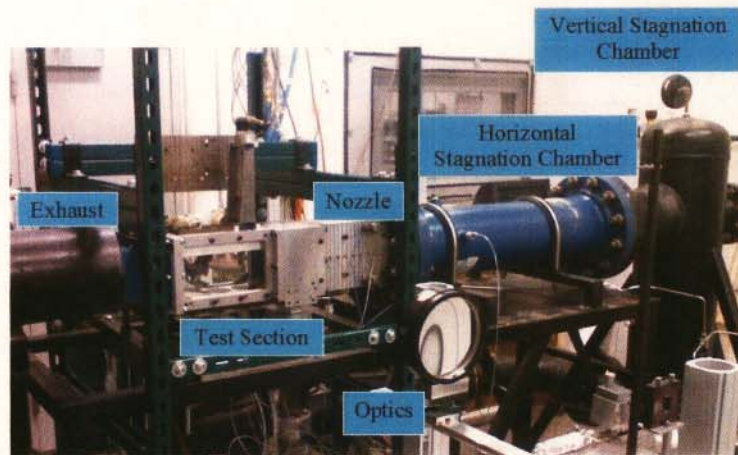
Figure 3: Picture of wind tunnel used in experiments

All experiments were conducted in a conventional blowdown supersonic wind tunnel at the Benn T Zinn Aerospace Combustion Laboratory in the Daniel Guggenheim School of Aerospace Engineering, Georgia Institute of Technology. The wind tunnel had a test section with a cross-sectional area of 8cm x 8cm and was run at a Mach number of 2.5 with the Mach number of the secondary stream being varied to achieve a range of convective Mach numbers from 0.1 to 1.3.
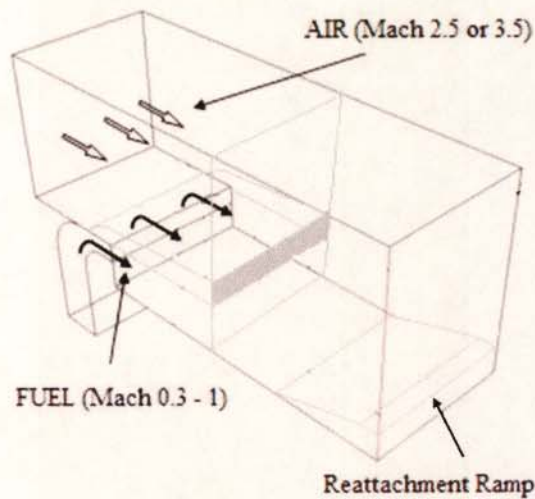
Figure 4: Schematic of test section

The secondary (fuel) stream was injected at a backward facing step, behind which the height of the test section increased to 10.54cm, resulting in an overall cross-sectional area increasing to 10.54 cm x 8 cm. This stream was injected parallel to the primary stream to prevent shocks when the two streams interact and mix. The downstream end of the test section featured a reattachment tamp. The stagnation pressure and temperature of the flow were varied between 0.41 MPa and 1.0 MPa and between 290K and 600K, respectively. A picture of the wind tunnel is shown in Figure 3 and a schematic of the test section is shown in Figure 4.

The top and bottom of the test section each had 3 circular ports of 70mm diameter on which quartz plugs were mounted to provide optical access and to attach wall pressure taps. Pressure transducers measured the wall pressure at a total of 51 stream-wise locations and the pressure distribution normal to the flow was measured using a probe mounted on a motorized traverse.

Schlieren Imaging System

A spark Schlieren system was used for flow visualization. A beam of light from a Xenon lamp, with a spark duration of 1 µs, was collimated, refocused on a pin hole and made to pass through the test section. A second lens then focused the beam on to a knife's edge and projected on to a screen, with the resulting image being captured by a Photron high speed camera (FASTCAM SA 3). A schematic of the system is shown in Figure 5.
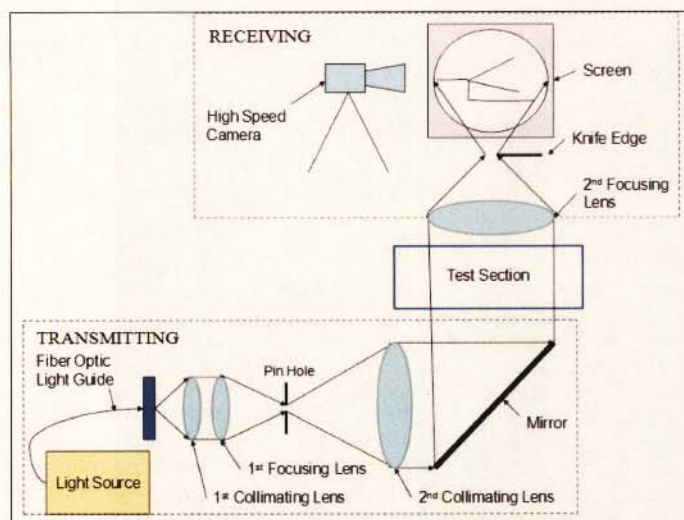
Figure 5: Schematic of Schlieren imaging system

Acetone PLIF system

The degree of mixing in the shear layers is quantified using the Planar Laser Induced Fluorescence (PLIF) technique. The secondary (fuel) stream is seeded with acetone which, upon application of the laser, is caused to fluoresce. By imaging the test section and examining the degree of fluorescence, the quantity of mixed fluid was calculated. The laser used was a frequency quadrupled Nd:YAG laser (Continuum Powerlite 8000) which produces a 266 nm beam with a pulse energy of 100mJ and a pulse width of 10 ns at a 10 Hz repetition rate. The beam produced by the laser was reshaped into a sheet of dimensions 45 x 200 µm by a system of 2 lenses and 2 mirrors,

before it entered the test section. The mirrors used were dichroic mirrors and the lenses were a -400 mm cylindrical and a 1500 mm spherical lens. A schematic of the PLIF system is shown in Figure 6.
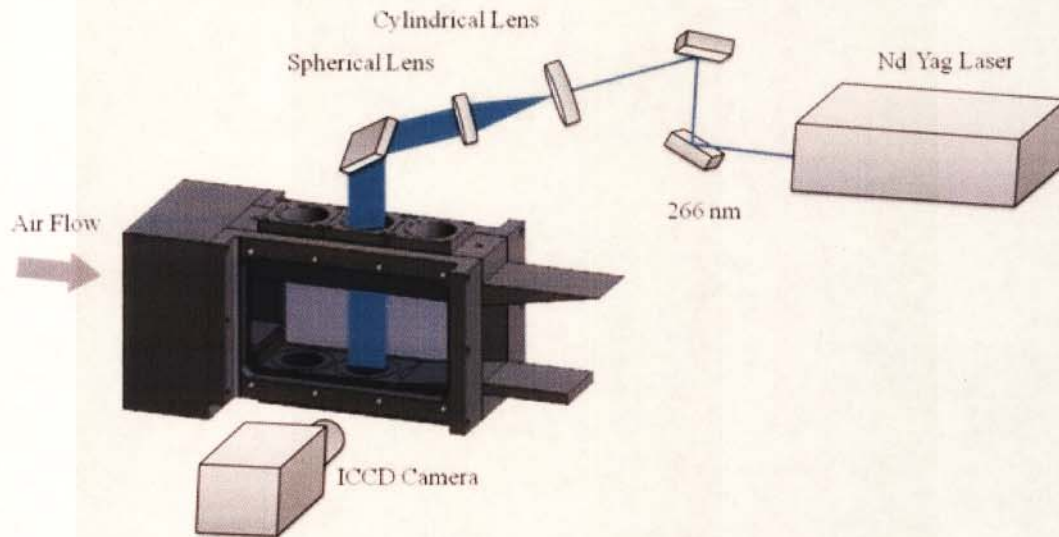
Figure 6: Schematic of the acetone PLIF system

The acetone fluorescence from the test section was imaged using an intensified CCD camera (Photron FASTCAM SA3, 1024 x 1024 array with 17 μm pixels), equipped with a Micro-Nikkor 55mm f/2.8 lens. This lens filters the scattered UV light (266 nm) while allowing the broadband fluorescence emission (350 to 550 nm) to pass through. The camera was set up such that it would be automatically triggered 10 ns after each pulse of the laser.

RESULTS

Preliminary Schlieren Results

Figures 7 through 10 show Schlieren results from 4 different preliminary runs conducted at different convective Mach numbers [12]. The convective Mach number was varied by injecting helium or nitrogen at Mach 1 into either a heated (530K) or an unheated air stream (300 K) at Mach 2.5. Figure 11 shows the shear layer growth rates for these 4 runs.
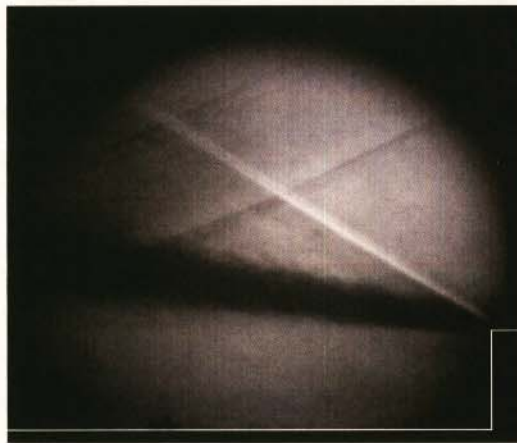
Figure 7: Helium and heated air (M_c = 0.09)

Figure 8: Helium & unheated air (M_c = 0.29)
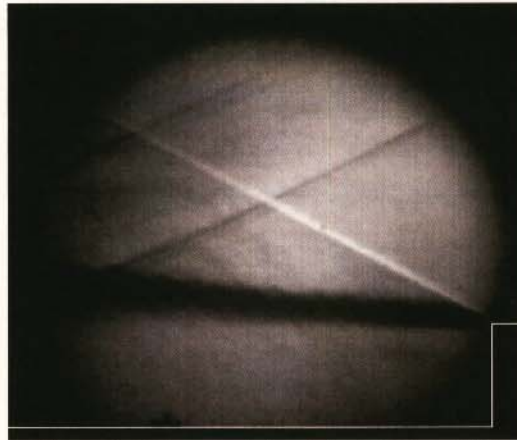
Figure 9: Nitrogen & heated air (Mc = 0.45)
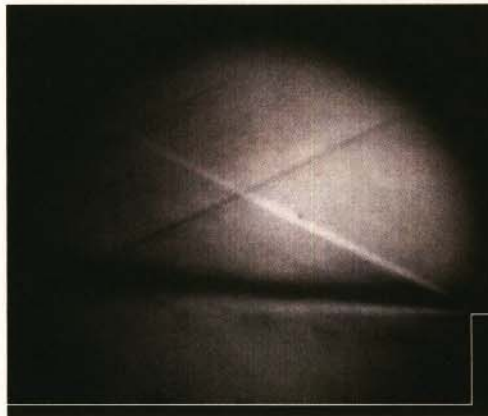
Figure 10: Nitrogen & unheated air (Mc = 0.73)
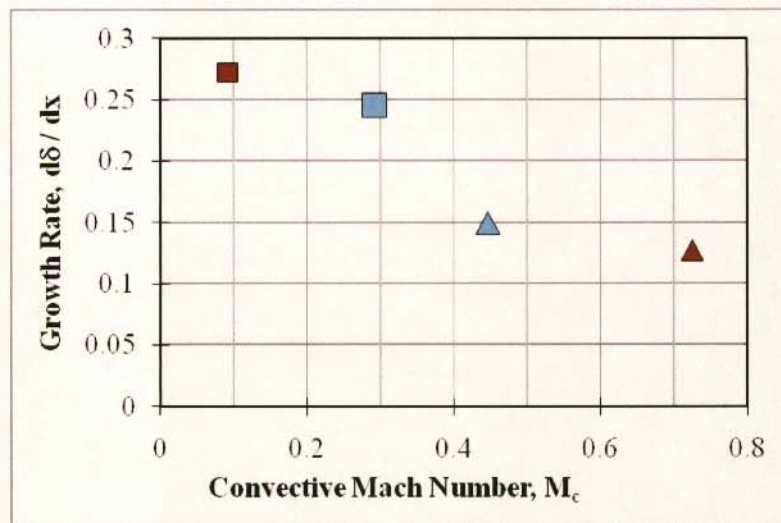
Figure 11: Scaling of growth rate with convective Mach number

11

Average Conditions

The average conditions measured during each of the 5 runs conducted are tabulated in Tables 1-5 (Appendix A). Data was acquired from 34 channels simultaneously at a frequency of 1000 Hz during all 5 runs. Tables 1-5 includes the means and standard deviations of the values measured by each channel at each of the 4 conditions (convective Mach numbers) that experiments were conducted at. A description of what each channel measured, along with the channel name, is provided in Table 6, below:

Table 6: Description of measured channels

Channel Name	Description
Other 03 (psia)	Stagnation pressure - secondary stream
Other 02 (psia)	Upstream static pressure - secondary stream
TS1 X-01 B (psia)	Test section static pressure - plug 1, tap 1
TS1 X-09/Z-09 B (psia)	Test section static pressure - bottom, z direction
1 (psia)	Upstream static pressure - primary stream
NS 1 (mV)	Photodiode voltage
SC (psia)	Pressure in vertical stagnation chamber - primary stream
NS 4 (psia)	Nozzle section static pressure at throat
3 (psia)	Differential pressure - primary stream
2 (psia)	Upstream static pressure of secondary stream
4 (psia)	Differential pressure - secondary stream
To He (°C)	Stagnation temperature - secondary stream
T Other (°C)	Upstream static temperature - acetone
T He (°C)	Upstream static temperature - secondary stream

Mass Flow Rate Calculations

The mass flow rates of air and acetone were calculated using the iterative method outlined below[13], and are tabulated in Tables 7-11 (Appendix B), corresponding to runs 1 through 5, respectively:

(i) Initially, assume discharge coefficient, C = 0.6

(ii) Make initial guess for mass flow rate:

$$\dot{m} = \left(\frac{\pi}{4}\sqrt{2}\right)\frac{CY_1D_2{}^2}{\sqrt{1-\beta^4}}\sqrt{\rho\Delta P}$$

where D_2 = 0.036007 m and Y_1 = 0.9645

(iii) Calculate new discharge coefficient based on calculated mass flow rate guess:

$$R_D = \frac{\dot{m}}{\left(\frac{\pi}{4\mu D_2}\right)}$$

where μ = 1.84 x 10^{-5} Ns/m²

$$C = C_\infty + \frac{b}{R_D}$$

where $C_\infty = 0.5959 + 0.0312\left(\beta^{2.1}\right) - 0184(\beta^8)$ and
$b = 91.706(\beta^{2.5})$

(iv) Use C calculated in (iii) to calculate new mass flow rate, using the equation in (ii), which becomes the mass flow guess for the next iteration. Continue to iterate until ($\dot{m}_{guess}$ / $\dot{m}_{actual}$) – 1 < 0.000000000000001.

DISCUSSION

Preliminary Schlieren Results – Shear Layer Growth Rate

From figures 7 through 10, it is evident that, as the convective Mach number increases, the thickness of the shear layer decreases significantly. Therefore, the shear layer growth rate decreases with increasing convective Mach number. This is summarized in Figure 11. This result is in accordance with that reported by Bonanos et al.[9].

Average Conditions and Repeatability

The means of the test conditions measured are consistent with expectations and provide verification that the experiments were designed and conducted correctly. The experiments conducted were also highly repeatable, as evidenced by the low standard deviations of the mass flow rates of both streams and the acetone mole fraction (Tables 6-10, Appendix B).

Mass Flow Rates and Convective Mach Numbers

The mass flow rates calculated will be used, according to the following relation, to calculate the true convective Mach number, M_c, achieved during each run. An accurate measure of the convective Mach number actually achieved is vital to being able to establish a relationship between mixing efficiency and compressibility.

$$M_c = \frac{\Delta U}{a_1 + a_2}$$

14

REFERENCES

[1] Slessor, M, D., Zhuang, M and Dimotakis, P, E., "Turbulent Shear Layer Mixing: growth-rate compressibility scaling," Journal of Fluid Mechanics, Vol. 414, pp. 38, 2000.

[2] Papamoschous, D. and Roshko, A., "The Compressible Turbulent Shear Layer: An Experimental Study," Journal of Fluid Mechanics, Vol. 197, pp. 458-477, 1988.

[3] Rossmann, T., Mungal, M. G., Hanson, R. K., "Mixing Efficiency Measurements Using a Modified Cold Chemistry Technique," Experiments in Fluids, Vol. 37, pp. 566-576, 2004.

[4] Breidenthal, R.E., "Structure in turbulent mixing layers and wakes using a chemical reaction." J. Fluid Mech., Vol. 125, pp. 397–409, 1981.

[5] Sankaran, V. and Menon, S., "LES of scalar mixing in supersonic mixing layers," Proc. Comb. Inst., Vol. 30, pp. 2835-2842, 2005.

[6] Smits, A. J. and Dussauge, J. P., Turbulent Shear Layers in Supersonic Flow, 2nd Edition, New York, Springer, 2005, pp. 15-42, 139-178

[7] Brown, G.L. and Roshko, A., "On Density Effects and Large Structures in Turbulent Mixing Layers,"

[8] Bogdanoff, D.W., "Compressibility Effects in Turbulent Shear Layers," AIAA Journal, Vol. 21, No. 6, pp. 926-927, 1983

[9] Bonanos, A. M., Bergthorson, J. M., Dimotakis, P. E., "Molecular Mixing and Flowfield Measurements in Recirculating Shear Flow. Part II: Supersonic Flow," Flow Turbulence Combust, Feb. 2009

[10] Island, T.C., Urban, W.D., Mungal, M.G., "Quantitative scalar measurements in compressible mixing layers," AIAA Paper 1996-0685, Jan. 1996

[11] Mungal MG, Frieler CE "The effect of Damko¨hler number in a turbulent shear layer.", Combust Flame, pp. 71:23–34, 1988

[12] Lungu, C., "An Experimental Study of Mixing in Compressible Shear Layers," Ph.D. Thesis Proposal, Georgia Institute of Technology, Atlanta, GA, 2011 (unpublished).

[13] Miller, R.W., Flow Measurement Engineering Handbook, 3rd Edition, McGraw Hill, 1996

APPENDIX A

Table 1: Average Conditions for Run 1 (07/26/2012 – run 5)

	Other 03	Other 02	TS1 X-01 B	TS1 X-09/Z-09 B	1	NS 1	SC	NS 4	3	2	4	To He	T Other	T He
Condition 10.55														
Mean	10.3026	10.1076	5.552949	5.665728162	14.5	12.72533	101.4371	6.1535172	1.65605	25.09793	0.390925	37.98786	74.55862	40.7414
Standard Deviation	0.14348	0.1064	0.038514	0.041680894	0.172	0.172369	0.425744	0.1345444	0.09838	5.252654	0.37029	3.37667	5.473606	3.24961
Condition 8.85														
Mean	8.81595	8.67022	5.645032	5.747071894	12.13	12.64511	100.381	6.073544	1.37763	21.02642	0.356765	44.63245	69.3121	43.33
Standard Deviation	0.14189	0.09625	0.16072	0.156136833	0.185	0.173285	0.638559	0.1398922	0.06469	3.77126	0.343991	3.325746	5.125221	3.19191
Condition 7.69														
Mean	7.58746	7.49919	5.738227	5.816779296	9.679	12.56446	100.7097	6.087445	0.79504	19.51883	0.352996	48.93298	67.47143	44.2364
Standard Deviation	0.11722	0.06776	0.023943	0.029169572	0.192	0.173443	0.27425	0.1329849	0.05527	4.032306	0.266446	3.230516	5.283187	3.17891
Condition 6.75														
Mean	6.7935	6.75169	5.717672	5.772224636	7.984	12.47272	101.2048	6.1177831	0.46095	17.22488	0.33205	51.09533	63.33624	44.5617
Standard Deviation	0.09077	0.04683	0.029544	0.033616006	0.155	0.176177	0.291013	0.136015	0.04814	3.210302	0.24169	3.150305	5.443013	3.14579

Table 2: Average Conditions for Run 2 (07/26/2012 – run 6)

	Other 03	Other 02	TS1 X-01 B	TS1 X-09/z-09 B	1	NS 1	SC	NS 4	3	2	4	To He	T Other	T He
Condition 6.75														
Mean	6.776057	6.707025	5.630270233	5.73583107	7.7405	12.8044	101.6381	6.164584	0.3802	36.2125	0.39044	44.9358	74.82744	36.95319
Standard Deviation	0.081505	0.068443	0.042326162	0.04639853	0.1459	0.165824	0.707064	0.135018	0.0394	3.52099	0.28944	3.90358	4.095736	3.150361
Condition 7.69														
Mean	7.619813	7.530308	5.638969189	5.76663102	9.2535	12.73837	100.7534	6.091049	0.5347	35.9095	0.35858	50.223	77.50745	39.39604
Standard Deviation	0.067702	0.073435	0.0249848	0.03012211	0.1248	0.169657	0.316652	0.130451	0.0573	1.95946	0.30256	3.29829	3.585151	3.193472
Condition 8.85														
Mean	8.787839	8.673836	5.608017899	5.71697981	11.506	12.67182	100.7988	6.088332	1.0172	36.8603	0.35634	54.6089	78.87359	41.00297
Standard Deviation	0.036636	0.035066	0.027756209	0.02994673	0.0954	0.17283	0.290126	0.131622	0.0637	0.89798	0.3122	3.46139	3.237602	3.2323
Condition 10.55														
Mean	10.47115	10.27941	5.480064971	5.62875175	14.238	12.59436	100.288	6.056907	1.4283	35.9425	0.29706	58.4019	78.83183	42.9503
Standard Deviation	0.059238	0.034303	0.027211827	0.02916449	0.0988	0.173381	0.275443	0.132268	0.0739	1.72928	0.32528	3.31574	3.307977	3.279646

Table 3: Average Conditions for Run 3 (07/27/2012 - run 2)

	Other 03	Other 02	TS1 X-01 B	TS1 X-09/Z-09 B	1	NS 1	SC	NS 4	3	2	4	To He	T Other	T He
Condition 6.75														
Mean	6.817804	6.79687	5.7065224	5.858555	7.797193	12.92071	101.6591	6.175848	0.3843	35.6946	0.37935	45.97065	75.04623	35.78439
Standard Deviation	0.084251	0.05653	0.0368102	0.036785	0.145713	0.15096	0.563311	0.118787	0.03779	3.44705	0.29748	3.703024	4.100565	2.910764
Condition 7.69														
Mean	7.514237	7.42465	5.7561582	5.864458	9.108881	12.85978	101.0452	6.111526	0.57137	35.4091	0.33426	51.19705	78.04741	38.45841
Standard Deviation	0.104494	0.08491	0.0266932	0.027958	0.171833	0.155381	0.336695	0.119803	0.06162	3.07148	0.29988	3.046378	4.48805	2.950507
Condition 8.85														
Mean	9.001017	8.9154	5.9215051	5.993926	11.80664	12.72684	100.9544	6.09746	1.05844	36.6291	0.22919	57.84392	79.60829	41.11413
Standard Deviation	0.122823	0.04626	0.3518241	0.340422	0.102246	0.158739	0.258181	0.121906	0.04559	0.87148	0.32373	3.069718	3.054422	3.020695
Condition 10.55														
Mean	10.31563	10.0568	5.8368979	5.886338	14.13066	12.62631	104.4572	6.330755	1.38905	35.604	0.37415	55.4678	83.76037	39.60951
Standard Deviation	0.096434	0.09449	0.0472372	0.045431	0.110137	0.167404	0.526627	0.13227	0.09242	3.87209	0.3735	4.316924	4.928835	3.836869

Table 4: Average Conditions for Run 4 (07/28/2012 - run 2)

	Other 03	Other 02	TS1 X-01 B	TS1 X-09/Z-09 B	1	NS 1	SC	NS 4	3	2	4	To He	T Other	T He
Condition 6.75														
Mean	6.903421	6.809614	6.28433	6.271302	7.7444	12.9991	104.9567	6.344641	0.3038	32.5946	0.28351	45.34143	80.03845	34.71452
Standard Deviation	0.09835	0.094563	0.057912	0.059582	0.1623	0.153158	0.764329	0.123325	0.04673	4.33009	0.31678	3.877362	5.395649	3.264573
Condition 7.69														
Mean	7.729279	7.573462	6.467417	6.431129	9.3785	12.86982	100.2859	6.037115	0.48235	33.6653	0.5154	53.97029	82.64309	37.14678
Standard Deviation	0.091498	0.087099	0.029668	0.033013	0.1542	0.157043	0.252317	0.117546	0.0529	2.66872	0.25007	3.014776	3.699254	2.829171
Condition 8.85														
Mean	8.962397	8.793789	7.43845	7.383156	11.199	12.75906	100.2691	6.035295	0.88887	33.8673	0.50712	58.96081	82.69038	38.34985
Standard Deviation	0.278057	0.317041	0.495755	0.490624	0.1833	0.153517	0.238179	0.115182	0.04561	2.49261	0.27291	2.877755	3.631202	2.778714
Condition 10.55														
Mean	10.55459	10.32364	8.121624	8.070892	13.884	12.6736	97.91319	5.90468	1.35107	33.8209	0.4968	62.05234	82.35017	39.31868
Standard Deviation	0.157046	0.181843	0.428267	0.421484	0.1063	0.153694	3.037544	0.20577	0.09286	2.06355	0.27561	3.052867	3.459267	2.794371

4

Table 5: Average Conditions for Run 5 (07/28/2012 - run 3)

	Other 03	Other 02	TS1 X-01 B	TS1 X-09/Z-09 B	1	NS 1	SC	NS 4	3	2	4	To He	T Other	T He
Condition 10.55														
Mean	10.58836	10.47299	7.323568	7.031527	14.69366	13.13232	103.2221	6.230478	1.452298	32.53928	0.435026	48.08314	81.65068	35.48961
Standard Deviation	0.108469	0.109178	0.043392	0.042425	0.127157	0.150777	0.653185	0.116934	0.088546	4.095386	0.346402	3.670684	4.669081	2.905117
Condition 8.85														
Mean	8.646421	8.583462	7.244917	7.134505	10.9002	12.91794	100.8587	6.066375	0.752417	32.89919	0.49942	60.22684	82.24816	40.1062
Standard Deviation	0.315997	0.345398	0.465122	0.501386	0.217706	0.1549	0.260598	0.114825	0.041085	2.848694	0.308946	2.928602	3.778304	2.804001
Condition 7.69														
Mean	7.689937	7.633189	6.58091	6.486584	9.52303	12.75232	101.4173	6.102682	0.482845	33.06917	0.341143	63.6266	81.96559	40.77528
Standard Deviation	0.07924	0.077863	0.029314	0.029966	0.139381	0.152748	0.240744	0.113637	0.051071	2.678471	0.243999	2.840593	3.657489	2.775369
Condition 6.75														
Mean	7.268445	7.224238	6.661411	6.578462	8.100223	12.6102	89.25806	5.396411	0.221577	33.48051	0.341117	65.97264	81.56376	41.09651
Standard Deviation	1.085997	1.072293	1.050718	1.098785	0.94142	0.154183	7.173457	0.447512	0.065722	2.955158	0.241684	3.00567	4.039696	2.787536
Condition 6.75 (before pressure drops)														
Mean	6.714464	6.681868	6.229992	6.1106	7.529416	12.64673	100.878	6.076492	0.219944	29.45338	0.313909	64.6308	77.5914	41.10806
Standard Deviation	0.034671	0.035929	0.021573	0.027855	0.102242	0.151293	0.344371	0.113463	0.059571	1.26019	0.242319	2.782143	2.92536	2.786969

Table 7: Mass Flow Rates (kg/s) for Run 1 (07/26/2012 - run 5)

	$\dot{m}_{air}$	$\dot{m}_{acetone}$	$\dot{m}_{total}$	Acetone Mole Fraction
Condition 10.55				
Mean	0.11043	0.02246	0.132887	0.089258
Standard Deviation	0.00281	0.01293	0.012699	0.049493
Condition 8.85				
Mean	0.09188	0.01967	0.111547	0.093201
Standard Deviation	0.00193	0.01133	0.011372	0.051503
Condition 7.69				
Mean	0.0632	0.01933	0.082529	0.128003
Standard Deviation	0.0021	0.00943	0.009698	0.058352
Condition 6.75				
Mean	0.04423	0.01772	0.061956	0.160831
Standard Deviation	0.00217	0.00826	0.008443	0.069255

Table 8: Mass Flow Rates (kg/s) for Run 2 (07/26/2012 - run 6)

	$\dot{m}_{air}$	$\dot{m}_{acetone}$	$\dot{m}_{total}$	Acetone Mole Fraction
Condition 6.75				
Mean	0.040223	0.027355	0.067577358	0.24120857
Standard Deviation	0.002005	0.01256	0.012737144	0.09882152
Condition 7.69				
Mean	0.05161	0.025711	0.077321372	0.18969993
Standard Deviation	0.00267	0.012983	0.013226137	0.08848599
Condition 8.85				
Mean	0.078031	0.025793	0.103824001	0.1360232
Standard Deviation	0.002433	0.013432	0.01366558	0.06696393
Condition 10.55				
Mean	0.101877	0.023023	0.124899696	0.09738675
Standard Deviation	0.00247	0.013956	0.014102516	0.05682073

Table 9: Mass Flow Rates (kg/s) for Run 3 (07/27/2012 - run 2)

	$\dot{m}_{air}$	$\dot{m}_{acetone}$	$\dot{m}_{total}$	Acetone Mole Fraction
Condition 6.75				
Mean	0.04066	0.02665	0.0673087	0.233747
Standard Deviation	0.001931	0.01284	0.0129827	0.101484
Condition 7.69				
Mean	0.052894	0.02455	0.0774469	0.17867
Standard Deviation	0.002775	0.01309	0.0133836	0.088563
Condition 8.85				
Mean	0.080575	0.02031	0.1008898	0.105663
Standard Deviation	0.001671	0.01421	0.0143065	0.070968
Condition 10.55				
Mean	0.10068	0.02558	0.1262589	0.108272
Standard Deviation	0.003047	0.01477	0.0147324	0.060063

Table 10: Mass Flow Rates (kg/s) for Run 4 (07/28/2012 - run 2)

	$\dot{m}_{air}$	$\dot{m}_{acetone}$	$\dot{m}_{total}$	Acetone Mole Fraction
Condition 6.75				
Mean	0.036217	0.02159	0.057807	0.212205
Standard Deviation	0.002853	0.013384	0.013647	0.121155
Condition 7.69				
Mean	0.049669	0.031101	0.080771	0.233295
Standard Deviation	0.002685	0.009085	0.009512	0.058985
Condition 8.85				
Mean	0.072562	0.030654	0.103216	0.170384
Standard Deviation	0.001639	0.010071	0.010207	0.050721
Condition 10.55				
Mean	0.098522	0.030242	0.128764	0.130414
Standard Deviation	0.003256	0.010247	0.010641	0.041322

2

Table 11: Mass Flow Rates (kg/s) for Run 5 (07/28/2012 - run 3)

	$\dot{m}_{air}$	$\dot{m}_{acetone}$	$\dot{m}_{total}$	Acetone Mole Fraction
Condition 10.55				
Mean	0.105627	0.026896	0.132522	0.109543
Standard Deviation	0.002874	0.013202	0.013057	0.051343
Condition 8.85				
Mean	0.06599	0.029588	0.095578	0.17764
Standard Deviation	0.001646	0.011361	0.011487	0.062226
Condition 7.69				
Mean	0.0498	0.024276	0.074075	0.188494
Standard Deviation	0.002523	0.010727	0.011003	0.076364
Condition 6.75				
Mean	0.031111	0.024474	0.055585	0.270738
Standard Deviation	0.004288	0.010722	0.011535	0.107344
Condition 6.75 (before pressure drops)				
Mean	0.030089	0.021954	0.052043	0.255011
Standard Deviation	0.004099	0.010299	0.011123	0.109665